Journal of Nuclear Medicine, published on May 5, 2022 as doi:10.2967/jnumed.121.263470

^{89}Zr-DFO-durvalumab PET/CT prior to durvalumab treatment in patients with recurrent or metastatic head and neck cancer

Sarah R. Verhoeff, MD[1], Pim P. van de Donk, MD[2], Erik H.J.G. Aarntzen, MD PhD[3], Sjoukje F. Oosting, MD PhD[2], Adrienne H. Brouwers, MD PhD[4], Iris H.C. Miedema, MD[5], Jens Voortman MD PhD[5], Willemien C. Menke-van der Houven van Oordt, MD PhD[5], Ronald Boellaard, MD PhD[3,6], Dennis Vriens, MD PhD[7], Marije Slingerland, MD PhDh[8], Rick Hermsen, MD[9], Ilse van Engen-van Grunsven, MD PhD[10], Sandra Heskamp, MD PhD[3*], Carla M.L. van Herpen, MD PhD[1*]

[1] Department of Medical Oncology, Radboud University Medical Center, Nijmegen, the Netherlands
[2] University of Groningen, University Medical Center Groningen, Department of Medical Oncology, Groningen, the Netherlands
[3] Department of Radiology and Nuclear Medicine, Radboud University Medical Center, Nijmegen, the Netherlands
[4] University of Groningen, University Medical Center Groningen, Department of Nuclear Medicine and Molecular Imaging, Groningen, the Netherlands
[5] Amsterdam UMC, Vrije Universiteit Amsterdam, Department of Medical Oncology, Cancer Center Amsterdam, the Netherlands
[6] Amsterdam UMC, Vrije Universiteit Amsterdam, Department of Radiology and Nuclear Medicine, Cancer Center Amsterdam, the Netherlands
[7] Department of Radiology, section of Nuclear Medicine, Leiden University Medical Center, the Netherlands
[8] Department of Medical Oncology, Leiden University Medical Center, the Netherlands
[9] Department of Nuclear Medicine, Canisius Wilhelmina Hospital, Nijmegen, the Netherlands
[10] Department of Pathology, Radboud University Medical Center, Nijmegen, the Netherlands

*joined last authorship

Running title: PD-L1 PET-imaging in SCCHN

Financial support: This study was funded by AstraZeneca, Radboud Institute for Health Sciences, NWO (91617039, KWF (10099).

Corresponding author: Prof. C.M.L. van Herpen, MD, PhD

Radboud University Medical Center Nijmegen, Department of Medical Oncology, P.O. Box 9101, 6500 HB Nijmegen, The Netherlands. Phone (+31) 243614038; Fax (+31) 243615025; E-mail: Carla.vanherpen@radboudumc.nl

ABSTRACT

Background

In the PINCH study we performed ^{89}Zr-DFO-durvalumab (anti-PD-L1) PET/CT in patients with recurrent or metastatic squamous cell carcinoma of the head and neck (SCCHN) prior to monotherapy durvalumab treatment. The primary aims were to assess safety and feasibility of ^{89}Zr-DFO-durvalumab PET-imaging and predict disease control rate during durvalumab treatment. Secondary aims were to correlate ^{89}Zr-DFO-durvalumab uptake to tumor PD-L1 expression, ^{18}F-FDG uptake, and treatment response of individual lesions.

Methods

In this prospective multicenter phase I-II study (NCT03829007), patients with incurable R/M SCCHN underwent baseline ^{18}F-FDG PET and CT or MRI imaging. Subsequently, PD-L1 PET-imaging was performed 5 days after 37MBq [^{89}Zr]Zr-DFO-durvalumab administration. To optimize imaging conditions, dose-finding was performed in the first 14 patients. For all patients, durvalumab treatment (1500mg/4 weeks, IV) was started <1 week after PD-L1 PET imaging and continued until disease progression or unacceptable toxicity (maximum 24 months). CT evaluation was assessed according to RECIST 1.1 every 8 weeks. PD-L1-expression was determined by combined positive score (CPS) on (archival) tumor-tissue. ^{89}Zr-DFO-durvalumab uptake was measured in ^{18}F-FDG-positive lesions, primary and secondary lymphoid organs, and bloodpool.

Results

In total, 33 patients with locoregional recurrent (n=12) or metastatic SCCHN (n=21) were enrolled. ^{89}Zr-DFO-durvalumab injection was safe. A dose of 10mg durvalumab resulted in highest tumor-to-blood-ratios. After a median follow-up of 12.6 months, overall response rate was 26%. The disease control rate at 16 weeks was 48% with a mean duration of 7.8 months (range 1.7-21.1). On a patient level, ^{89}Zr-DFO-durvalumab-SUV_{peak} or tumor-to-blood ratio could not predict treatment response (HR 1.5 (95%CI 0.5-3.9, p=0.45) and (HR 1.3 (95%CI 0.5-3.3,

p=0.60) respectively). Also, on a lesion level, ^{89}Zr-DFO-durvalumab-SUV_{peak} showed no substantial correlation to treatment response (Spearman ρ 0.45, *p*= 0.051). Lesional ^{89}Zr-DFO-durvalumab-uptake did not correlate to PD-L1 CPS score, but did correlate to ^{18}F-FDG SUV_{peak} (Spearman ρ 0.391, *p*= 0.005).

Conclusion

PINCH is the first PD-L1 PET/CT study in patients with R/M SCCHN and has shown the feasibility and safety of ^{89}Zr-DFO-durvalumab PET/CT in a multi-center trial. ^{89}Zr-DFO-durvalumab-uptake did not correlate to durvalumab treatment response.

Key words: PD-L1, ImmunoPET, head and neck cancer, immune checkpoint inhibitors, durvalumab

INTRODUCTION

Squamous cell carcinoma of the head and neck (SCCHN) is the seventh most common cancer worldwide, with up to 900,000 new diagnoses in 2020 (*1*). Patients with recurrent/metastatic (R/M) SCCHN with no curative options have a poor prognosis (*2*). However, a subset of patients derives durable responses from immune checkpoint inhibitors (ICI) targeting Programmed cell death 1 (PD-1) or its ligand (PD-L1) (*3-5*), although selecting those patients upfront remains challenging.

Patients who benefit most from ICI often express high levels of tumor PD-L1 as analysed by immunohistochemistry, using different assays, scoring protocols and cut-offs (*5-8*). Since June 2019, pembrolizumab received FDA and EMA-approval as 1st line treatment of R/M SCCHN patients with an immunohistochemistry combined positive score (CPS) of at least ≥1. Thus, pre-treatment assessment of PD-L1 has major clinical implication, although there are also patients with a PD-L1 negative tumor biopsy who benefit from ICI (*9-11*).

Therefore, there is a clinical need to better understand ICI responses and the caveats that remain with selection based on PD-L1 expression in tumor biopsies. The role and expression of PD-L1 in anti-cancer immune responses is complex and warrants a biomarker that enables monitoring its heterogenous and dynamic expression in different (tumor) tissues (*12*). Molecular imaging with radiolabeled tracers targeting PD-1/PD-L1 allows non-invasive visualization of all accessible PD-1/PD-L1 (*13,14*). This approach overcomes important limitations of immunohistochemistry analyses, including invasive biopsies and sampling errors (*15,16*). It is a complementary tool to blood and tissue sampling, potentially providing relevant information for patient selection and to steer drug development (*17*).

The first clinical PD-1/PD-L1 imaging studies were performed with ^{89}Zr-labeled atezolizumab (anti-PD-L1) and nivolumab (anti-PD-1) in patients with metastatic breast cancer, bladder cancer and non-small cell lung cancer (NSCLC), demonstrating a correlation between

tracer-uptake and treatment response (*18,19*). So far, no PD-L1 PET imaging studies have been performed in patients with R/M SCCHN.

The primary aim of the PD-L1 ImagiNg to prediCt durvalumab treatment response in SCCHN (PINCH) study was to assess the safety and feasibility of ^{89}Zr-DFO-durvalumab PD-L1 PET imaging and to predict durvalumab disease control rate in patients with R/M SCCHN. Secondary aims were to investigate the correlation of ^{89}Zr-DFO-durvalumab uptake to 1) PD-L1 expression measured on tumor biopsies, 2) ^{18}F-FDG uptake and 3) treatment response of individual tumor lesions.

MATERIALS AND METHODS

Patients

Eligible patients were aged ≥18 years, had an Eastern Cooperative Oncology Group (ECOG) performance status of 0 or 1, and a life expectancy of at least 12 weeks. Patients had histologically or cytologically confirmed R/M SCCHN of the oral cavity, oropharynx, hypopharynx, or larynx not amenable to curative therapy, with no prior systemic treatment for R/M SCCHN. Patients with known leptomeningeal carcinomatosis, symptomatic or uncontrolled brain metastases requiring treatment, were excluded. Patient recruitment was performed in four university medical centers in the Netherlands (Radboudumc, UMC Groningen, Amsterdam UMC and Leiden UMC). The study was performed in accordance with the Declaration of Helsinki and approved by the institutional review board of each participating center.

Procedures

Contrast-enhanced (ce)CT and/or MRI, ^{18}F-FDG PET/CT and ^{89}Zr-DFO-durvalumab PET/CT

At baseline, all patients underwent ceCT and/or MRI of the head and neck, chest and abdomen, combined with whole-body ^{18}F-FDG PET/CT and ^{89}Zr-DFO-durvalumab PET/CT. ^{18}F-FDG PET/CT was performed according to European Association of Nuclear Medicine (EANM) guidelines version 1.0 (*20*) and the ^{89}Zr-imaging procedure was harmonized between participating EARL-accredited centers (PET/CT-systems) (*21*). Patients underwent ^{89}Zr-DFO-durvalumab PET/CT 5 days after intravenous (IV) injection of ~37 MBq ^{89}Zr-DFO-durvalumab. Details on, conjugation, radiolabeling and quality control of ^{89}Zr-DFO-durvalumab and image acquisition and reconstruction are described in the supplements (*21-24*).

After baseline imaging, all patients were planned for durvalumab treatment (fixed dose of 1500mg iv once every 4 weeks) starting within one week after PET-imaging until disease progression or unacceptable toxicity, for a maximum of 24 months. Data on adverse events was collected up to 90 days after the last treatment dose and graded according to the National Cancer Institute Common Terminology Criteria for Adverse Events (CTCAE version 4.0). Treatment evaluation was performed with ceCT of the head and neck, chest and abdomen at baseline and every 8 weeks during treatment, using Response Evaluation Criteria in Solid Tumors (RECIST) version 1.1. Participants were contacted every 3 months to assess survival after discontinuation of durvalumab treatment.

^{89}Zr-DFO-durvalumab PET/CT

Dose finding

Based on prior dose finding studies with ^{89}Zr-labeled antibodies, we aimed to enrol a minimum of 3 patients per dose cohort (2, 10 or 50 mg durvalumab) (*25*). All patients received an intravenous injection of 2mg ^{89}Zr-DFO-durvalumab. For the 10 and 50mg cohort, ^{89}Zr-DFO-durvalumab was complemented with 8 and 48 mg unlabelled durvalumab, respectively. For pharmacokinetic purposes, blood plasma samples were drawn within 10 minutes after injection

and five days later (day of the PET scan). Plasma radioactivity was measured in a gamma counter and reported as the percentage injected dose (%ID/g). The optimal dose for ^{89}Zr-DFO-durvalumab PET-imaging was determined based on pharmacokinetic blood analyses and visual and quantitative PET analyses.

After dose finding, we aimed to include an additional 43 patients receiving the optimal dose ^{89}Zr-DFO-durvalumab. However, the study was closed early for enrolment in December 2020 due to the registration of pembrolizumab as 1st line treatment for R/M SCCHN patients in the Netherlands (June 2020). In total, we enrolled an additional 19 patients who underwent the same procedures as described above, except for the collection of blood samples for pharmacokinetic analyses.

Imaging assessment

ceCT and/or MRI and ^{18}F-FDG PET/CT. Baseline ceCT/MRI and ^{18}F-FDG PET/CT-scans were centrally reviewed by two independent radiology and nuclear medicine physicians (E.H.J.G.A., R.H.), according to standard clinical practice. The evaluation of CT lesions was performed according to RECIST 1.1 (*26*). Lesion size was defined as the mean size in millimetres (mm) as determined by two reviewers.

The ^{18}F-FDG PET/CT-scans were assessed using the PET Response Criteria in Solid Tumors (PERCIST) criteria (*27*). A tumor lesion was defined visually positive based on anatomical substrate on low-dose CT in combination with higher than surrounding ^{18}F-FDG-uptake, and a diameter on ceCT or MRI of ≥10mm or ≥15mm in lymph nodes (*26*). The maximum and peak standardized uptake values (SUV) based on body weight were obtained, as well as metabolic tumor volume (MTV) and total lesion glycolysis (TLG).

^{89}Zr-DFO-durvalumab PET/CT. The quantification of tumor lesions was performed by placing a 3D sphere in a ^{18}F-FDG-positive lesions using Accurate tool software developed in IDL version 8.4 (Harris Geospatial Solutions, Bloomfield, USA)) (*28*). This was done for all ^{18}F-FDG-positive lesions, irrespective of visual ^{89}Zr-DFO-durvalumab uptake. This volume of interest (VOI) was manually delineated around the entire lesion if this could be distinguished from the background. In tumor lesions without evident visual zirconium-89 uptake, a spherical VOI of 1cm3 was drawn at the anatomical location of the tumor lesion, based on the low dose CT, diagnostic CT and ^{18}F-FDG PET/CT. On a lesion level, the SUV_{peak} of individual lesions were determined to report tumor tracer-uptake. For healthy organs and blood pool, SUV_{mean} was reported. To correct for variable concentrations of circulating ^{89}Zr-DFO-durvalumab, tumor-to-blood (TTB) ratios were reported as SUV_{peak} tumor/ SUV_{mean} blood. The blood pool activity was measured in a spherical VOI in the descending aorta. To correct for differences in number of lesions per patient, the lesional SUV_{peak} and ^{18}F-FDG TLG values of one individual patient were summarized as geometric mean (gm) values. This was used to correlate tracer-accumulation to treatment response. Furthermore, to correct for partial volume effect, subgroup analyses were performed for lesions ≥20m (reported in the supplementals)

PD-L1 immunohistochemistry

Fresh or archival cytological or histological samples suitable for PD-L1 staining was available for 27 patients. This involved tumor tissue from recurrent disease (n=12), or metastases in lung (n=7), lymph node (n=7) or bone (n=1). PD-L1 staining was performed using VENTANA PD-L1 (SP263) assay and evaluated by a certified pathologist in head and neck cancer (I.E.), blinded for clinical information. As an internal control, staining for PD-L1 was performed with the clinical validated 22C3 antibody using the DAKO stainer in histological samples of 8 patients (*8*). In all samples, PD-L1 expression was assessed according to the combined positive score (CPS), which describes the number of PD-L1 positive tumor cells plus

immune cells per 100 tumor cells, showing positive cell membrane staining and/or a score of <1, 1-20 or >20.

Statistical analyses

Clinical outcome was evaluated according to an intention-to-treat analyses on a patient and lesion level. This was visualized in a waterfall plot. Furthermore, we assessed the disease control rate (DCR), overall response rate (ORR), progression free survival (PFS) and overall survival (OS). A log-rank test was performed to correlate PD-L1 CPS to PFS. A Cox regression model was used to report hazard ratios (HR) for progressive disease.

In the dose finding study, we compared differences in tracer-uptake and TTB ratios between the three dose groups, testing for significance using a two-sided Kruskal-Wallis test.

On a patient level, the relation between ^{89}Zr-DFO-durvalumab, patient gm SUV_{peak} and SUV_{peak} of the hottest lesion with durvalumab response was explored by Kaplan–Meier survival plots. Similar analyses were performed for gm ^{18}F-FDG SUV_{peak}, TLG and MTV. Patients were grouped in a below-median and above-median group to evaluate a difference in survival using the log-rank test. The relation between these groups was tested by additional Cox regression models, reporting HRs for progressive disease and/or survival.

We correlated ^{89}Zr-DFO-durvalumab uptake with ^{18}F-FDG SUV_{peak} and ^{18}F-FDG TLG on a lesion level. Additional descriptive analyses were performed to evaluate the per lesion PD-L1 expression to tracer accumulation. For these correlations we report the Spearman correlation coefficient (ρ). Statistical analysis were performed using SPSS Statistics for windows version 22.0. Differences with a p-value of 0.05 or less were considered statistically significant.

RESULTS

Baseline characteristics

Between April 2019 and December 2020, 37 patients were screened, three were considered ineligible and one declined to participate. ^{89}Zr-DFO-durvalumab PET dose finding was performed in 14 patients (supplemental, Figure 1). 21/33 (64%) patients presented with metastatic disease, most frequently located in lung (45%) and lymph nodes (39%). PD-L1 CPS scores could be determined in 27 patients (82%), including 17 patients with only archival tumor tissue available. Baseline characteristics are reported in Table 1.

Durvalumab treatment

In total, 31/33 patients started durvalumab treatment. Two patients showed rapid disease progression before treatment initiation and were offered best supportive care. One other patient showed rapid disease progression before first disease evaluation at 8 weeks. After a median follow-up of 12.6 months, the median time on durvalumab treatment was 5.3 months (range 1.2-26.5).

The median PFS was 5.3 months (95%CI 2.96-7.62) and median OS was 13.1 months (95%CI 7.88-18.40). The survival rate at 12 and 24 months was 58% (95%CI 8.82-11.28) and 45% (95%CI: 8.91-24.87), respectively (Supplemental Figure 2). The ORR was 26%, including three patients with complete response and five patients with partial response. The best response to durvalumab treatment per patient is depicted in Figure 1. The DCR at 16 weeks was 48% with a mean response duration of 7.8 months (range 1.7-21.1). The most frequent reported grade 3-4 treatment-related adverse events were elevated ALT/AST caused by hepatitis, and pneumonitis *(*Supplemental Table 1*).* PD-L1 CPS scores showed no association with PFS (PFS of 4.6 vs 12.9 vs 3.5 months with CPS scores <1, 1-20 and >20, respectively (p=0.259*,* Supplemental Figure 3).

^{89}Zr-DFO-durvalumab PET/CT dose finding

In total, 14 patients were assigned to one of three dose cohorts: 2mg (n=4), 10mg (n=6), or 50mg (n=4) durvalumab. No clinically relevant infusion-related reactions for the injection with ^{89}Zr-DFO-durvalumab were reported.

Example ^{89}Zr-DFO-durvalumab PET/CT-scans are shown in Figure 2. The PK-analysis at day 5 showed lowest ^{89}Zr-DFO-durvalumab (%ID/g) plasma concentration in the 2mg cohort (Supplemental Figure 4), while highest concentrations were measured in the 50mg cohort (p=0.077). Dose cohort 10mg showed variable plasma concentrations between patients. In the 2mg cohort, tumor lesions could not be visualized properly and high tracer retention was observed in the liver and the spleen. At higher antibody doses, liver and spleen uptake decreased and tumor uptake increased. Also, increasing antibody dose resulted in visually prolonged ^{89}Zr-DFO-durvalumab circulation time. Quantitative analyses showed that mean TTB ratio was highest in the 10mg cohort and lowest in cohort 50mg (cohort 2mg: 2.28±0.61, cohort 10mg: 3.75±0.93, cohort 50mg: 1.48±1.64; p=0.019, Supplemental Figure 5).

Based upon the highest TTB ratios, and tumor visualization, we selected 10mg for subsequent ^{89}Zr-DFO-durvalumab PET/CT imaging.

PET-imaging analyses

In total, 24 patients underwent ^{89}Zr-DFO-durvalumab PET/CT-imaging using an antibody dose of 10 mg. In these patients, ^{89}Zr-DFO-durvalumab tumor accumulation was measured for all ^{18}F-FDG positive tumor lesions (n=53). The ^{89}Zr-DFO-durvalumab uptake, lesion size and lesion location are displayed in Figure 3. An overview of all lesions can be found in Supplemental Table 2.

^{89}Zr-DFO-durvalumab PET imaging. For quantitative analyses of ^{89}Zr-DFO-durvalumab, 53 lesions were included. No significant differences were observed between lesions in different

organ sites. However, accumulation of ^{89}Zr-DFO-durvalumab was highly variable in tumor lesions within and between patients, which is illustrated in Figure 3 and 4. The largest heterogeneity in one patient was observed between a lung (SUV_{peak} 3.3) and liver (SUV_{peak} 9.8) metastasis. Highest SUV_{peak} values were reported in two bone lesions (SUV_{peak} 13.4 and SUV_{peak} 13.6) and one locoregional lymph node (SUV_{peak} 12.2). ^{89}Zr-DFO-durvalumab SUV_{peak} was correlated with lesion size (Spearman ρ 0.359, *p*= 0.09) and ^{18}F-FDG SUV_{peak} (Spearman ρ 0.391, p=0.005), but not with organ site (Spearman ρ 0.15, *p*= 0.28). The overall mean gm ^{89}Zr-DFO-durvalumab SUV_{peak} was 6.0 (95%CI 4.6-7.3).

^{18}F-FDG PET imaging. In 33 patients, 70 ^{18}F-FDG-positive lesions were identified according to PERCIST criteria used for quantitative analyses. The ^{18}F-FDG uptake was highly variable within and between patients, with overall gm ^{18}F-FDG SUV_{peak} 7.7 (range 2.0-18.2) and ^{18}F-FDG TLG 70.3 ml (range 2.7-659.0 ml).

Correlation between tracer uptake and treatment response or PD-L1 expression

^{89}Zr-DFO-durvalumab PET/CT

The median PFS of patients with an above median ^{89}Zr-DFO-durvalumab SUV_{peak} was 5.7 months compared to 3.5 months in the below median group (HR 1.5 (95%CI 0.5-3.9, *p*=0.45, Figure 5A). Also, gm ^{89}Zr-DFO-durvalumab TTB ratio did not correlate with survival (HR 1.3 (95%CI 0.5-3.3, *p*=0.60) (Figure 5B). Patients grouped based on the hottest lesion, showed a similar PFS of 5.7 months (SUV_{peak} ≥6.22) vs. 3.5 months (SUV_{peak} <6.22) (HR 1.1 (95%CI 0.4-3.0, *p*= 0.84)).

To correct for partial volume effect, the correlation of ^{89}Zr-DFO-durvalumab SUV_{peak} and TTB ratio with PFS was also performed after correcting for lesions <20mm, showing no essential differences between results described for all lesions (Supplemental Figure 6).

In total, 35 lesions were visible on evaluation CT scans during treatment. On a lesion level, ^{89}Zr-DFO-durvalumab accumulation and treatment response was variable (Figure 6). There was no substantial correlation between lesional ^{89}Zr-DFO-durvalumab SUV_{peak} or TTB ratio with the change in lesion size at 12 weeks (Spearman ρ 0.45, *p*= 0.051 and Spearman ρ -0.669, *p*= 0.78, respectively). A cut-off of the median SUV_{peak} of these lesions did not improve the correlation of 89Zr-DFO-durvalumab SUV_{peak} with treatment response (Spearman ρ 0.67, p=0.855).

^{18}F-FDG PET/CT

Patients with an above median ^{18}F-FDG TLG showed a significantly worse outcome compared to patients with a low ^{18}F-FDG TLG (median PFS 1.8 versus 7.3 months, HR 2.4 (95%CI 1.1-5.4, p=0.04, Figure 7). Patients with above median ^{18}F-FDG SUV_{peak} showed a median PFS of 5.3 compared to 5.7 months in the below median group (HR 1.5 (95%CI 0.7-3.4, p=0.30). The ^{18}F-FDG MTV was not associated with PFS (p=0.69) (not shown).
The correlation between ^{18}F-FDG SUV_{peak} and ^{18}F-FDG TLG ratio with PFS after correcting for lesions <20mm is reported in supplements and showed similar results as described for all lesions (Supplemental Figure 7).

On a lesion level, PD-L1 CPS score did not correlate to ^{89}Zr-DFO-durvalumab SUV_{peak} (Spearman ρ 0.38, *p*= 0.20), ^{89}Zr-DFO-durvalumab TTB ratio (Spearman ρ -0.06, p=0.85), ^{18}F-FDG TLG (Spearman ρ 0.40, *p*= 0.90) or ^{18}F-FDG SUV_{peak} (Spearman ρ -0.12, *p*= 0.70).

DISCUSSION

The PINCH study reported ^{89}Zr-DFO-durvalumab PET/CT in R/M SCCHN patients treated with durvalumab to address current caveats in the predictive role of PD-L1 expression on tumor biopsies. ^{89}Zr-DFO-durvalumab PET/CT was considered safe and feasible in a multi-

center setting. Heterogenous ^{89}Zr-DFO-durvalumab tumor accumulation was detected within and between patients. ^{89}Zr-DFO-durvalumab uptake could not predict durvalumab treatment response.

To achieve optimal tumor-to-background contrast, selection of proper antibody dose and imaging timing is essential. The PINCH study showed superior TTB ratios when performing PET/CT 5 days after ^{89}Zr-DFO-durvalumab administration using 10 mg of durvalumab, compared with 2 and 50 mg. In agreement with previous studies, increasing the dose of unlabeled antibody saturates the spleen uptake and results in higher concentrations of circulating ^{89}Zr-labeled antibodies and increased tumor uptake (*24,25*). At 50 mg, TTB ratio decreased, most likely explained by a decrease in available binding sites for ^{89}Zr-DFO-durvalumab. In line with this, low or absent tumor accumulation was also reported for ^{89}Zr-DFO-durvalumab PET-imaging with 750 mg unlabelled durvalumab (*22*).

Preclinical studies have demonstrated a relation between the accumulation of radiolabeled PD-(L)1 antibodies with PD-L1 expression, thereby distinguishing between tumors with different PD-L1 expression levels (*13,14*). The first two clinical trials also reported an association between radiolabeled PD-L1 antibody uptake and PD-L1 expression (*18,19*). However, we did not find such a correlation. Of note, our analysis was performed on a subset of patients using archival tissue biopsies, as fresh histologic prove was not mandatory for study inclusion. Besides sampling error due to small tumor samples, correlating (archival) biopsies to PET-imaging remains challenging due to the heterogenous and dynamic expression levels of PD-L1. Also, in comparison to previous studies, the PD-L1 staining and scoring procedures differed (*29,30*).

A previous study in 22 patients with metastatic NSCLC, triple negative breast cancer and bladder cancer treated with atezolizumab, above median gm ^{89}Zr-atezolizumab SUV_{max} was associated with improved overall and progression free survival (*18*). Furthermore, both ^{89}Zr-

nivolumab (anti PD-1) and ^{18}F-BMS-986192 (anti PD-L1) SUV_{peak} were correlated to nivolumab treatment response in 13 NSCLC patients. However, two other studies using ^{89}Zr-durvalumab and ^{89}Zr-pembrolizumab in NSCLC patients, showed a trend but no significant correlation between tracer-uptake and durvalumab respectively pembrolizumab treatment efficacy (*22,31*), which is more in line with our data. The early termination of the study resulted in a lower number of included patients. Potentially, more patients could have resulted in a significant correlation. We also evaluated the correlation between tumor metabolism and ICI response, as performed in previous studies (*32,33*). Our data suggests that particularly ^{18}F-FDG total lesion glycolysis may identify poor durvalumab responders upfront. A potential explanation could be that patients with more extensive disease have already undergone extra steps in the immune escape route.

Altogether, PET-imaging with ^{89}Zr-labeled PD-L1 antibodies has not consistently shown a correlation between tracer-uptake and treatment response. Potential explanations are the different characteristics of the antibodies used, which include 1) affinity for PD-L1 which could influence tumor retention; 2) Fc-tail modification/glycosylation which could affect circulation time and effector functions; 3) non-specific antibody-uptake due to enhanced permeability and retention (EPR) effect (*34-36*). As a result of the EPR-effect, there is always a (low) PET-signal in the tumor, while this is not PD-L1 mediated. This may hamper the detection of small amounts of tumor PD-L1, which can be clinically relevant as low PD-L1 expression (1% positive cells) has been associated with ICI response. To limit the non-specific-uptake and thereby increase the potential to measure low PD-L1 expression levels, small molecules or peptides with rapid blood clearance can be used (*37,38*). Finally, other mechanisms within immune suppressive microenvironment beyond PD-L1, such as the activation and promoting of CD8+ T-cell priming in tumor draining lymph nodes determine ICI response could have influenced the correlation between tracer-uptake and ICI response(*39*).

Despite the fact that ^{89}Zr-DFO-durvalumab did not correlate to treatment outcome, we do see potential of ^{89}Zr-labeled antibodies in optimizing the ICI treatment efficacy in patients with R/M SCCHN (*40*). Besides an unique insight in antibody biodistribution, the in vivo visualization of ^{89}Zr-labeled antibodies highlights essential local effector mechanisms, reveals the complexity of dose-response relations, and may shed a new light on the role of non-tumor located PD-L1 expression in the anti-cancer immune responses (*39*). Ultimately, this teaches us how to use (and combine) these drugs to improve response rates; an essential step in early drug development suitable for phase 1 and 2 clinical trials.

CONCLUSION

In conclusion, the PINCH study is the first to perform PD-L1 PET/CT in patients with R/M SCCHN. It has shown that ^{89}Zr-DFO-durvalumab PET/CT imaging is feasible and safe. However, ^{89}Zr-DFO-durvalumab uptake did not correlate to PD-L1 expression on a patient level and could not predict durvalumab treatment response.

Conflicts of interest: This study was supported by Astrazeneca.

CMLvH received research grants from AstraZeneca, Bristol-Myers Squibb, MSD, Merck, Ipsen, Novartis, and Sanofi. CMLvH has been on advisory boards for Bayer, Bristol-Myers Squibb, Ipsen, MSD, and Regeneron. EHJGA received research grant from AstraZeneca.

No other potential conflicts of interest relevant to this article exist.

Financial support: This study was funded by AstraZeneca, Radboud Institute for Health Sciences, NWO (91617039, KWF (10099).

KEY POINTS

QUESTION:	Can ^{89}Zr-DFO-durvalumab PET/CT predict durvalumab treatment in patients with recurrent or metastatic head and neck cancer?
PERTINENT FINDINGS:	This multi-center clinical trial studies the feasibility and safety of ^{89}Zr-DFO-durvalumab PET/CT and its ability to predict durvalumab treatment response. ^{89}Zr-DFO-durvalumab PET/CT was safe and feasible, but was unable to predict durvalumab treatment response.
IMPLICATIONS FOR PATIENT CARE	Our findings indicate that we need another approach than radiolabeled antibody based PET-imaging to predict treatment response to immune checkpoint inhibitors using molecular imaging.

REFERENCES

1. Sung H, Ferlay J, Siegel RL, et al. Global Cancer Statistics 2020: GLOBOCAN Estimates of Incidence and Mortality Worldwide for 36 Cancers in 185 Countries. *CA Cancer J Clin.* 2021;71:209-249.

2. Ferlay J, Colombet M, Soerjomataram I, et al. Estimating the global cancer incidence and mortality in 2018: GLOBOCAN sources and methods. *International Journal of Cancer.* 2018;144:1941-1953.

3. Harrington KJ, Ferris RL, Blumenschein G, Jr., et al. Nivolumab versus standard, single-agent therapy of investigator's choice in recurrent or metastatic squamous cell carcinoma of the head and neck (CheckMate 141): health-related quality-of-life results from a randomised, phase 3 trial. *Lancet Oncol.* 2017;18:1104-1115.

4. Cohen EEW, Bell RB, Bifulco CB, et al. The Society for Immunotherapy of Cancer consensus statement on immunotherapy for the treatment of squamous cell carcinoma of the head and neck (HNSCC). *J Immunother Cancer.* 2019;7:184.

5. Burtness B, Harrington KJ, Greil R, et al. Pembrolizumab alone or with chemotherapy versus cetuximab with chemotherapy for recurrent or metastatic squamous cell carcinoma of the head and neck (KEYNOTE-048): a randomised, open-label, phase 3 study. *The Lancet.* 2019;394:1915-1928.

6. Fridman WH, Pagès F, Sautès-Fridman C, Galon J. The immune contexture in human tumours: impact on clinical outcome. *Nature Reviews Cancer.* 2012;12:298.

7. Cohen EEW, Soulières D, Le Tourneau C, et al. Pembrolizumab versus methotrexate, docetaxel, or cetuximab for recurrent or metastatic head-and-neck squamous cell carcinoma (KEYNOTE-040): a randomised, open-label, phase 3 study. *The Lancet.* 2019;393:156-167.

8. de Ruiter EJ, Mulder FJ, Koomen BM, et al. Comparison of three PD-L1 immunohistochemical assays in head and neck squamous cell carcinoma (HNSCC). *Mod Pathol.* 2020.

9. Reck M, Rodriguez-Abreu D, Robinson AG, et al. Pembrolizumab versus Chemotherapy for PD-L1-Positive Non-Small-Cell Lung Cancer. *N Engl J Med.* 2016;375:1823-1833.

10. Rittmeyer A, Barlesi F, Waterkamp D, et al. Atezolizumab versus docetaxel in patients with previously treated non-small-cell lung cancer (OAK): a phase 3, open-label, multicentre randomised controlled trial. *The Lancet.* 2017;389:255-265.

11. Siu L, Even C, Mesía R, et al. A Randomized, Open-Label, Multicenter, Global Phase 2 Study of Durvalumab (D), Tremelimumab (T), or D Plus T, in Patients With PD-L1 Low/Negative Recurrent or Metastatic Head and Neck Squamous Cell Carcinoma: CONDOR. *International Journal of Radiation Oncology*Biology*Physics.* 2018;100:1307.

12. Verhoeff SR, van den Heuvel MM, van Herpen CML, Piet B, Aarntzen E, Heskamp S. Programmed Cell Death-1/Ligand-1 PET Imaging: A Novel Tool to Optimize Immunotherapy? *PET Clin.* 2020;15:35-43.

13. Heskamp S WPJ, Molkenboer-Kuenen J.C.M., et al. PD-L1 microSPECT/CT imaging for longitudinal monitoring of PD-L1 expression in syngeneic and humanized mouse models for cancer. *Cancer Immunology Research* 2018.

14. Hettich M, Braun F, Bartholoma MD, Schirmbeck R, Niedermann G. High-Resolution PET Imaging with Therapeutic Antibody-based PD-1/PD-L1 Checkpoint Tracers. *Theranostics.* 2016;6:1629-1640.

15. Hofman P. The challenges of evaluating predictive biomarkers using small biopsy tissue samples and liquid biopsies from non-small cell lung cancer patients. *J Thorac Dis.* 2019;11:S57-s64.

16. Kluger HM, Zito CR, Turcu G, et al. PD-L1 Studies Across Tumor Types, Its Differential Expression and Predictive Value in Patients Treated with Immune Checkpoint Inhibitors. *Clinical cancer research : an official journal of the American Association for Cancer Research.* 2017;23:4270-4279.

17. Waaijer SJH, Kok IC, Eisses B, et al. Molecular Imaging in Cancer Drug Development. *J Nucl Med.* 2018;59:726-732.

18. Bensch F, van der Veen EL, Lub-de Hooge MN, et al. (89)Zr-atezolizumab imaging as a non-invasive approach to assess clinical response to PD-L1 blockade in cancer. *Nat Med.* 2018;24:1852-1858.

19. Niemeijer AN, Leung D, Huisman MC, et al. Whole body PD-1 and PD-L1 positron emission tomography in patients with non-small-cell lung cancer. *Nat Commun.* 2018;9:4664.

20. Boellaard R, Delgado-Bolton R, Oyen WJ, et al. FDG PET/CT: EANM procedure guidelines for tumour imaging: version 2.0. *Eur J Nucl Med Mol Imaging.* 2015;42:328-354.

21. Makris NE, Boellaard R, Visser EP, et al. Multicenter harmonization of 89Zr PET/CT performance. *J Nucl Med.* 2014;55:264-267.

22. Smit J, Borm FJ, Niemeijer A-LN, et al. PD-L1 PET/CT imaging with radiolabeled durvalumab in patients with advanced stage non-small cell lung cancer. *Journal of Nuclear Medicine.* 2021.

23. Verel I, Visser GW, Boellaard R, Stigter-van Walsum M, Snow GB, van Dongen GA. 89Zr immuno-PET: comprehensive procedures for the production of 89Zr-labeled monoclonal antibodies. *J Nucl Med.* 2003;44:1271-1281.

24. Jauw YW, Menke-van der Houven van Oordt CW, Hoekstra OS, et al. Immuno-Positron Emission Tomography with Zirconium-89-Labeled Monoclonal Antibodies in Oncology: What Can We Learn from Initial Clinical Trials? *Front Pharmacol.* 2016;7:131.

25. Dijkers EC, Oude Munnink TH, Kosterink JG, et al. Biodistribution of 89Zr-trastuzumab and PET imaging of HER2-positive lesions in patients with metastatic breast cancer. *Clin Pharmacol Ther.* 2010;87:586-592.

26. Eisenhauer EA, Therasse P, Bogaerts J, et al. New response evaluation criteria in solid tumours: revised RECIST guideline (version 1.1). *Eur J Cancer.* 2009;45:228-247.

27. Pinker K, Riedl C, Weber WA. Evaluating tumor response with FDG PET: updates on PERCIST, comparison with EORTC criteria and clues to future developments. *Eur J Nucl Med Mol Imaging.* 2017;44:55-66.

28. Boellaard R. Quantitative oncology molecular analysis suite: ACCURATE. *Journal of Nuclear Medicine.* 2018;59:1753.

29. Madore J, Vilain RE, Menzies AM, et al. PD-L1 expression in melanoma shows marked heterogeneity within and between patients: implications for anti-PD-1/PD-L1 clinical trials. *Pigment Cell Melanoma Res.* 2015;28:245-253.

30. Ilie M, Long-Mira E, Bence C, et al. Comparative study of the PD-L1 status between surgically resected specimens and matched biopsies of NSCLC patients reveal major discordances: a potential issue for anti-PD-L1 therapeutic strategies. *Ann Oncol.* 2016;27:147-153.

31. Niemeijer AN, Oprea Lager DE, Huisman MC, et al. First-in-human study of (89)Zr-pembrolizumab PET/CT in patients with advanced stage non-small-cell lung cancer. *J Nucl Med.* 2021.

32. Dall'Olio FG, Calabro D, Conci N, et al. Baseline total metabolic tumour volume on 2-deoxy-2-[18F]fluoro-d-glucose positron emission tomography-computed tomography as a promising biomarker in patients with advanced non-small cell lung cancer treated with first-line pembrolizumab. *Eur J Cancer.* 2021;150:99-107.

33. Ito K, Schoder H, Teng R, et al. Prognostic value of baseline metabolic tumor volume measured on (18)F-fluorodeoxyglucose positron emission tomography/computed tomography in melanoma patients treated with ipilimumab therapy. *Eur J Nucl Med Mol Imaging.* 2019;46:930-939.

34. Boussiotis VA. Molecular and Biochemical Aspects of the PD-1 Checkpoint Pathway. *N Engl J Med.* 2016;375:1767-1778.

35. Arce Vargas F, Furness AJS, Litchfield K, et al. Fc Effector Function Contributes to the Activity of Human Anti-CTLA-4 Antibodies. *Cancer cell.* 2018;33:649-663.e644.

36. Shi Y, van der Meel R, Chen X, Lammers T. The EPR effect and beyond: Strategies to improve tumor targeting and cancer nanomedicine treatment efficacy. *Theranostics.* 2020;10:7921-7924.

37. Stutvoet TS, van der Veen EL, Kol A, et al. Molecular Imaging of PD-L1 Expression and Dynamics with the Adnectin-Based PET Tracer (18)F-BMS-986192. *J Nucl Med.* 2020;61:1839-1844.

38. Leung D, Bonacorsi S, Smith RA, Weber W, Hayes W. Molecular Imaging and the PD-L1 Pathway: From Bench to Clinic. *Front Oncol.* 2021;11:698425.

39. Borst J, Busselaar J, Bosma DMT, Ossendorp F. Mechanism of action of PD-1 receptor/ligand targeted cancer immunotherapy. *Eur J Immunol.* 2021;51:1911-1920.

40. Canning M, Guo G, Yu M, et al. Heterogeneity of the Head and Neck Squamous Cell Carcinoma Immune Landscape and Its Impact on Immunotherapy. *Front Cell Dev Biol.* 2019;7:52.

Figure legends

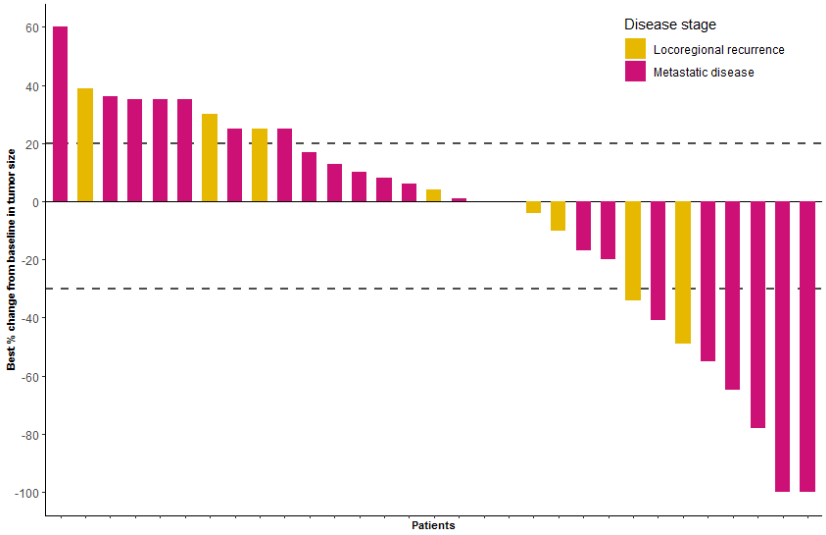

Figure 1 Waterfall plot**.** Each bar depicts the best response according to RECIST version 1.1 of a single patient during durvalumab treatment. Blue bars represent patients with metastatic disease; Pink bars patients with locoregional recurrent disease. Dotted lines reflect RECIST criteria for disease progression (+20% change) and partial response (-30%).

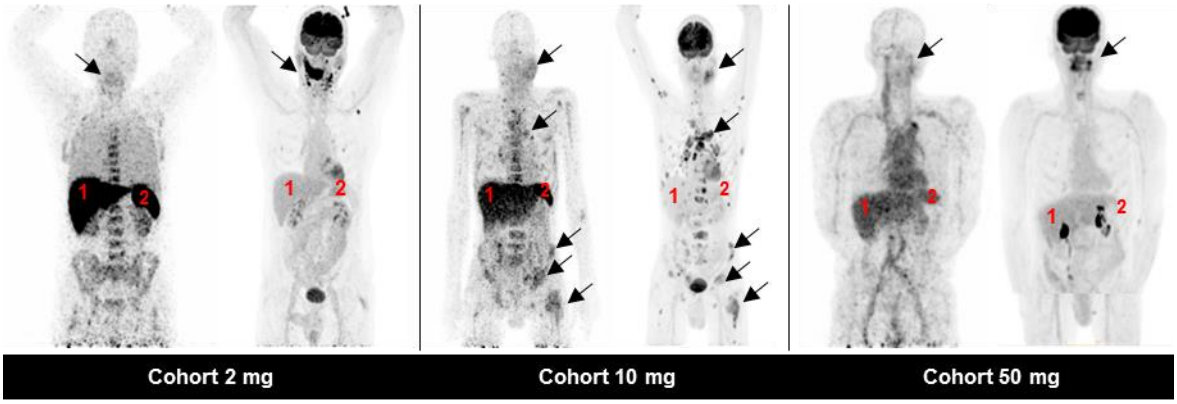

Figure 2. Representative examples images of one patient per dose cohort. For each cohort, the ^{89}Zr-DFO-durvalumab PET/CT (left) and ^{18}F-FDG PET/CT (right) are presented of one patient. Physiological ^{89}Zr-DFO-durvalumab is visualized in lymphoid organs (e.g. liver (1), spleen (2))**.** Tumor lesions are identified by arrows.

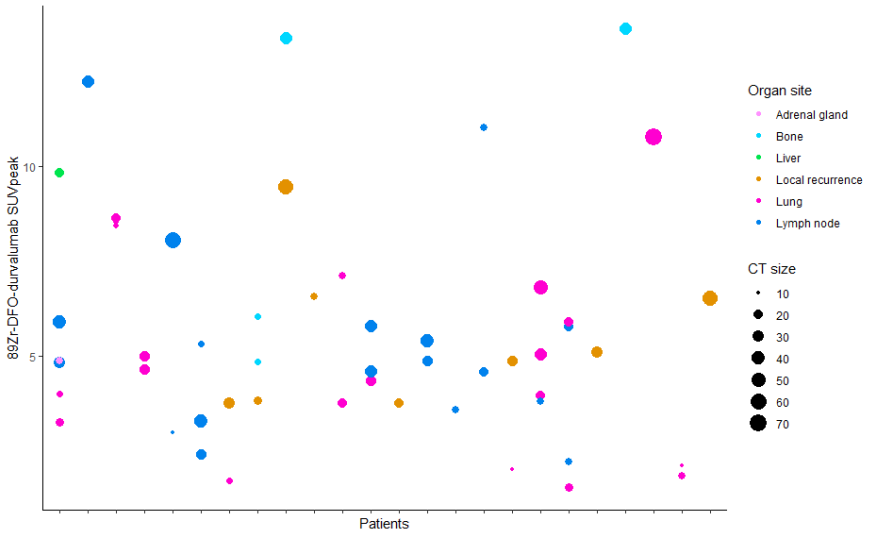

Figure 3 Scatterplot of all ^{18}F-FDG-positive lesions (n=53) measuring ≥10mm (or 15mm in lymph node) and their corresponding ^{89}Zr-DFO-durvalumab-uptake. Lesions were distributed over lung (n=20), lymph nodes (n=18), local recurrence (n=8), bone (n=5) and liver (n=1).

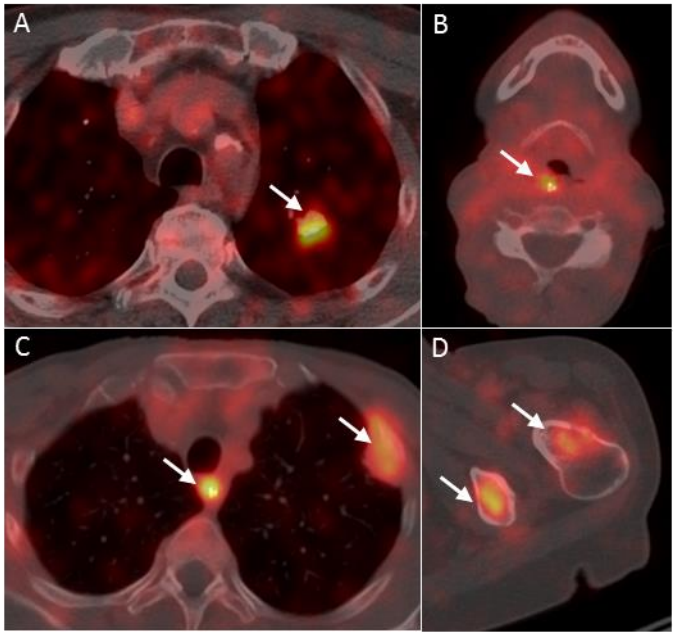

Figure 4 Example fused images of ^{89}Zr-DFO-durvalumab (10mg) PET/CT images showing tracer uptake in known tumor locations Displaying transversal sections in 4 different patients. The white arrows highlight tumor lesions in lung (A), local recurrence (B), lymph node and pleural lesion (C) and two other bone lesions (D)

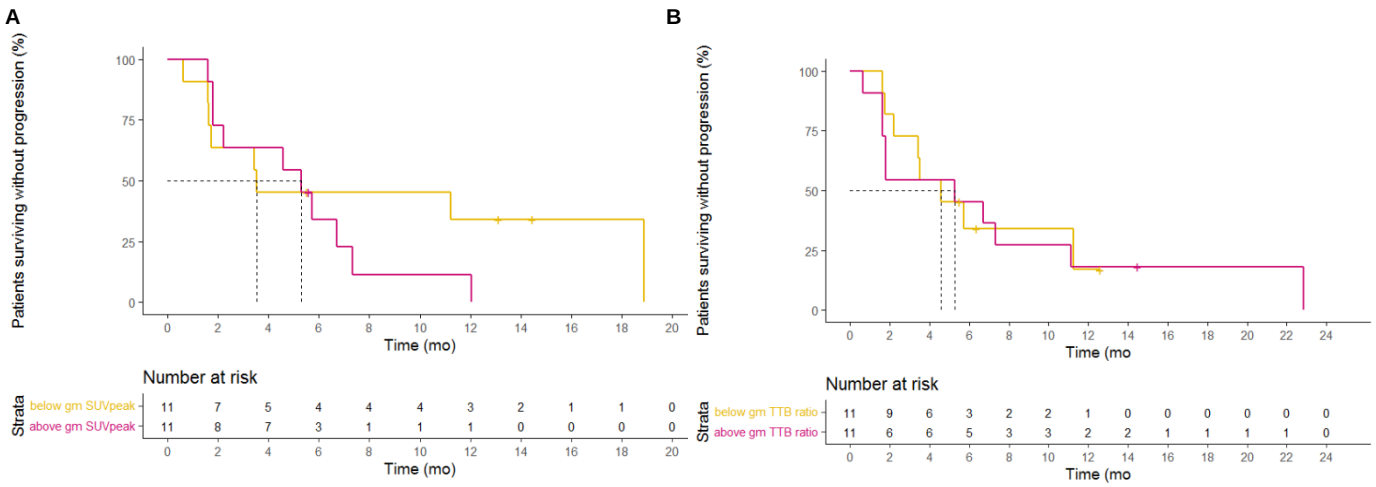

Figure 5. Kaplan-Meier estimates of progression free survival based on ^{89}Zr-DFO-durvalumab SUVpeak (A) and tumor-to-blood-ratios (B) dichotomized at median value

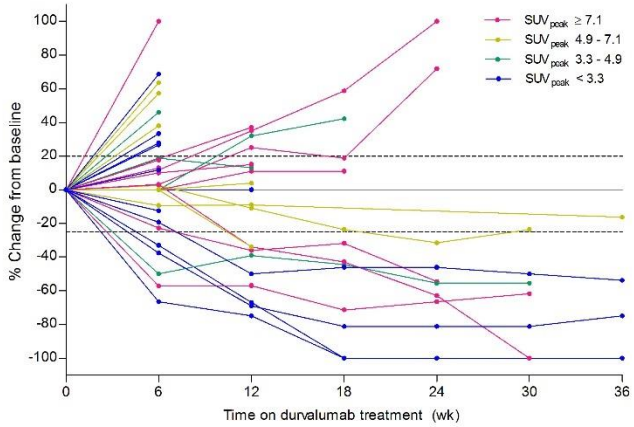

Figure 6. Spaghetti plot reporting lesional ^{89}Zr-DFO-durvalumab SUV_{peak} and lesional response of 17 lesions where colors identify the corresponding ^{89}Zr-DFO-durvalumab uptake by a distribution over quartiles.

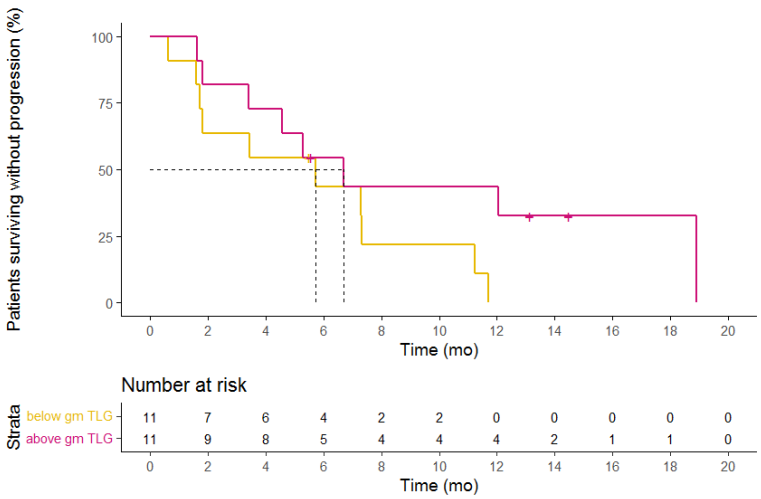

Figure 7. Kaplan-Meier estimates of progression free survival based on ^{18}F-FDG total lesion glycolysis dichotomized at the population median

Parameters	Patients (n=33)	
Age in years, median (range)	64.5	49-80
Sex, n(%)		
Male	26	(79%)
ECOG PS, n(%)		
0	10	(30%)
1	23	(70%)
Smoking, n(%)		
Current	4	(12%)
Never or former	29	(88%)
Alcohol, n(%)		
Current	24	(73%)
Never or former	9	(27%)
Primary tumor location, n(%)		
Hypopharynx	4	(13%)
Larynx	7	(22%)
Oral cavity	10	(30%)
Oropharynx	8	(24%)
Unknown	3	(10%)
Disease extent at baseline, n(%)		
Loco/regional recurrence	12	(36%)
Metastatic disease	21	(64%)
Location metastases		
Lung	28	(45%)
Lymph node	24	(39%)
Bone	5	(8%)
Other (Liver, adrenal gland, muscle)	4	(8%)
Prior treatments with curative intent*, n(%)		
Surgery alone	3	(9%)
Surgery with adjuvant radiation	8	(24%)
Surgery with adjuvant chemoradiation	9	(27%)
Radiation alone	5	(15%)
Chemoradiation	8	(24%)
Time from last platinum therapy, n(%)		
≤ 6 months	1	(6%)
> 6 months	16	(94%)
Histological/cytological biopsy**		
Archival	33	(70%)
Fresh	10	(30%)
PD-L1 status***, n(%)		
PD-L1 CPS <1	13	(40%)
PD-L1 CPS 1-20	8	(24%)
PD-L1 CPS ≥20	6	(18%)
No assessment possible	6	(18%)

Table 1. Baseline characteristics

ECOG PS, Eastern Cooperative Oncology Group performance status; PD-L1, programmed death ligand 1; CPS, combined positive score. Data are median (range) or n (%) *Chemotherapy regimen included monotherapy cisplatin or carboplatin, or combination regimens e.g. docetaxel, cisplatin and 5-fluorouracil or carboplatin and 5-fluorouracil ** A fresh biopsy was defined as histological or cytological tumor biopsy performed at study enrolment up to <1 months before study enrolment
***PD-L1 assessment was performed on biopsy tissue from recurrent or metastatic disease. PD-L1 staining was performed using the Ventana SP263.

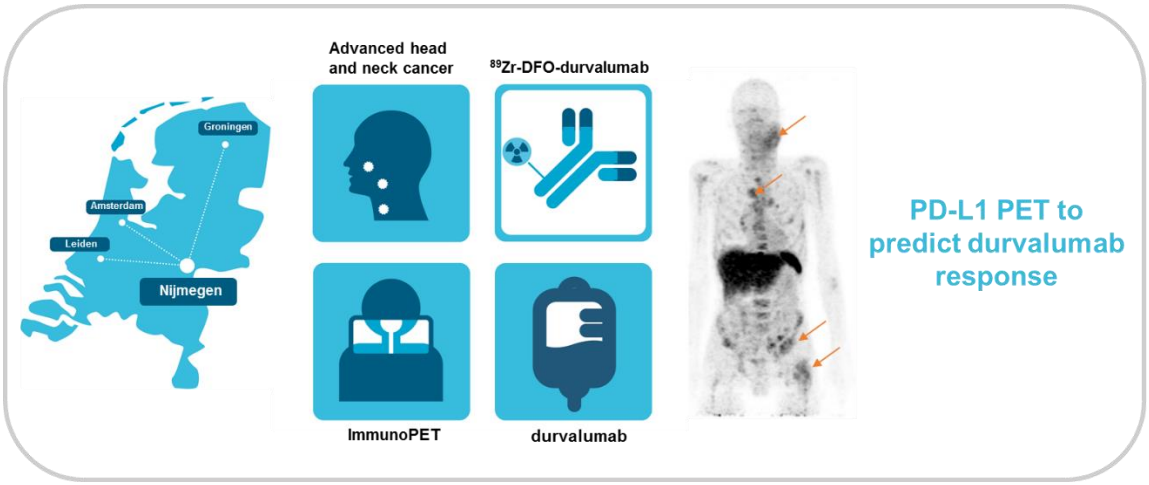

Graphical abstract

Supplements

Participating centers

Patients were enrolled in the Radboud university medical center (UMC) (n=13), UMC Groningen (n=10), Amsterdam UMC (n=6) and Leiden UMC (n=4).

Patient imaging

Contrast-enhanced CT-scan

The CT acquisition and reconstructions were performed according to local protocols for Canon Aquilion One GENESIS Edition (RadboudUMC & Leiden UMC), Siemens Force/Flash (UMC Groningen) scanner, Discovery CT750 (Amsterdam UMC).

Acquisition protocols were as follows;100 or 120 kV protocol (automatic exposure control (AEC) with standard deviation (SD) of 15), with auto mA 120-500, noise index of 25, at a rotation speed of 0.275-0.5 sec. Scan range included chest and abdomen. Reconstruction was performed by the Canon Aquilion scanner using adaptive iterative dose reduction 3dimensional enhance (AIDR 3Denh) in combination with FC08 filter to create axial in 1mm/0.8mm and axial, coronal and sagittal in 5mm/4mm slices and FC86 filter to create axial in 1mm/0.8mm and axial in 5mm/4mm and 10/3 MIP axial. Images from the Flash/Force scanner were reconstructed using SAFIRE iterative reconstructions programme 2 to create 1mm slices with an increment of 0.7mm for chest reconstructions and 2mm slices with an increment of 1,5mm in slices of the abdomen and pelvis. CT images of the Discovery CT750 were reconstructed using the adaptive statistical iterative reconstruction (ASIR) algorithm at 60-70% to create 0.625 mm axial and coronal slices of the chest and 3mm slices of the abdomen and pelvis. Image analysis was performed on the venous

phase scans after intravenous injection of iodinated contrast at 100-150 ml/kg body weight with bolus tracking at a delay of 30-80 sec (chest - abdomen) and maximal slice thickness of 5.0 mm.

Patient imaging – PET/CT

The ^{89}Zr-imaging procedure was harmonized between participating, EARL-accredited centers (PET/CT-systems) (*1*).

Patients underwent ^{89}Zr-DFO-durvalumab PET/CT 5 days after intravenous (IV) injection of ±37 MBq ^{89}Zr-DFO-durvalumab. For both PET/CT scans, patients were scanned from the head to upper thigh in up to 6 consecutive bed positions, during 5 minutes for each bed position with a 64-slice PET/CT camera (Siemens Biograph mCT, in RadboudUMC, Philips Gemini TF or Philips Ingenuity TF in UMC Groningen and Philips Vereos in Amsterdam UMC and Leiden UMC). All data were corrected for dead time, scatter, randoms, decay and tissue attenuation, with a final reconstruction resolution of 7 mm.

Conjugation, radiolabeling and quality control of ^{89}Zr-DFO-durvalumab

^{89}Zr-DFO-durvalumab was produced under good manufacturing practice (GMP) conditions.
Recently, one study has reported the conjugation and ^{89}Zr-labeling of DFO-durvalumab as performed for the individual patient (*2*). Due to the larger sample size of the PINCH study, we performed the conjugation of DFO-durvalumab as a bulk at the Radboudumc.

For the process of ^{89}Zr-labeling, durvalumab (AstraZeneca, Cambridge, England) was conjugated with the bifunctional chelator tetrafluorophenol-N-succinyldesferal-Fe(III) (TFP-N-SucDf or DFO; ABX, Radeberg, Germany) using 200 mg durvalumab and a 2-fold molar excess of DFO (*3*).

To remove unconjugated DFO, the conjugated DFO-durvalumab was purified using disposable gel permeation columns (PD10, GE Healthcare Life sciences, Eindhoven, The Netherlands).

Subsequent dilution with NaCl 0.9% resulted in a final concentration 2.5 mg/ml which was filtered through 0.22 µm Millex GV filter and dispensed.

Radiolabeling of DFO-durvalumab with ^{89}Zr was performed under GMP conditions at RadboudUMC and transported to participating centers. The radiolabeling process is performed at pH 7.2. To achieve the desired pH value, oxalic acid, sodium carbonate and HEPES buffer (adjusted to pH 7.3 by use of sodium hydroxide solution) are added(*3*). After addition of the conjugated mAb DFO-Durvalumab and HEPES buffer, radiolabeling is allowed to take place during 30 minutes at room temperature. .

After radiolabeling, purification is performed to remove the oxalic acid and HEPES. This purification takes place by use of a disposable PD10 column and NaCl 0.9% as eluent. The final radiolabeled product contains a total volume of 10 ml with a concentration of durvalumab (^{89}Zr-DFO-durvalumab + unlabelled non-conjugated durvalumab) according to the assigned dose cohort. The unlabelled antibody is added to prevent possible splenic uptake of the radiolabeled antibody (*4*). The final product contains ~37 MBq ^{89}Zr-DFO-durvalumab at the time of injection.

The radiochemical purity (as checked by thin layer chromatography and high performance liquid chromatography) was ≥95%. Specifically bound fraction of radiolabeled DFO-durvalumab was determined during validation using a binding assay performed in triplicate with a fixed MDA-MB-231 cell concentration, including controls for non-specific binding. The ratio of total bound activity divided by the non-specifically bound activity was always ≥2.

REFERENCES

1. Makris NE, Boellaard R, Visser EP, et al. Multicenter harmonization of 89Zr PET/CT performance. *J Nucl Med.* 2014;55:264-267.

2. Smit J, Borm FJ, Niemeijer A-LN, et al. PD-L1 PET/CT imaging with radiolabeled durvalumab in patients with advanced stage non-small cell lung cancer. *Journal of Nuclear Medicine.* 2021.

3. Verel I, Visser GW, Boellaard R, Stigter-van Walsum M, Snow GB, van Dongen GA. 89Zr immuno-PET: comprehensive procedures for the production of 89Zr-labeled monoclonal antibodies. *J Nucl Med.* 2003;44:1271-1281.

4. Jauw YW, Menke-van der Houven van Oordt CW, Hoekstra OS, et al. Immuno-Positron Emission Tomography with Zirconium-89-Labeled Monoclonal Antibodies in Oncology: What Can We Learn from Initial Clinical Trials? *Front Pharmacol.* 2016;7:131.

Supplemental figures and tables

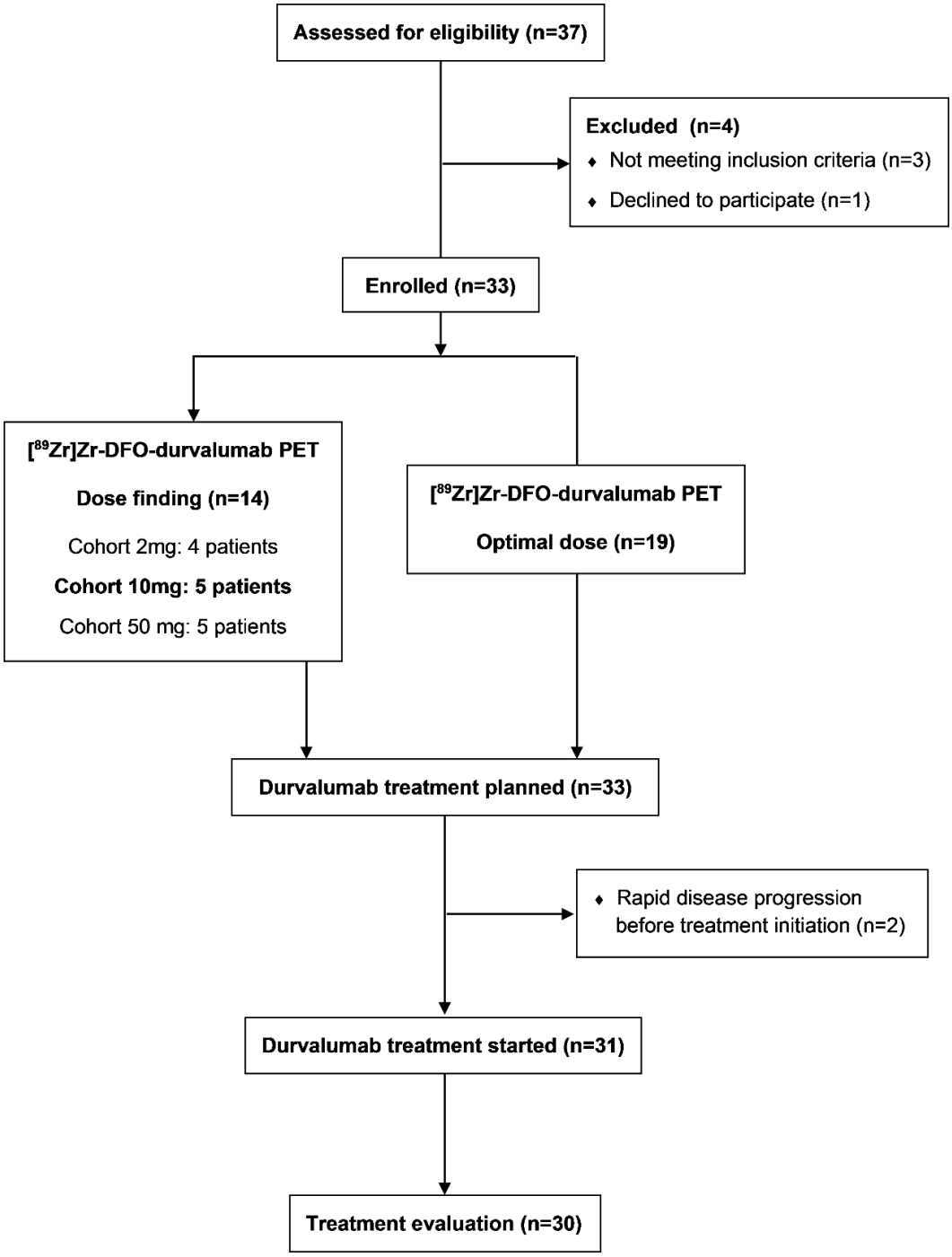

Figure 1. Flow-diagram of patient enrollment.

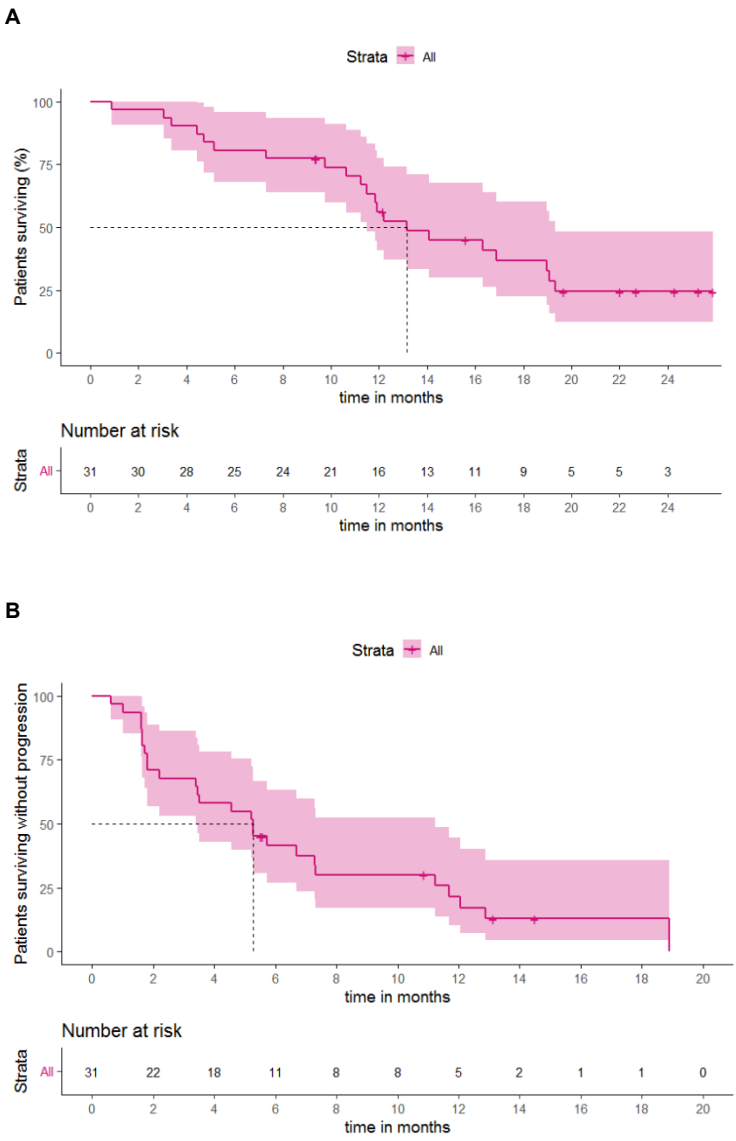

Figure 2. Kaplan-Meier estimates of the overall survival and progression free survival
The overall survival (A) and progression free survival (B) are displayed for all 31 patients treated with durvalumab.

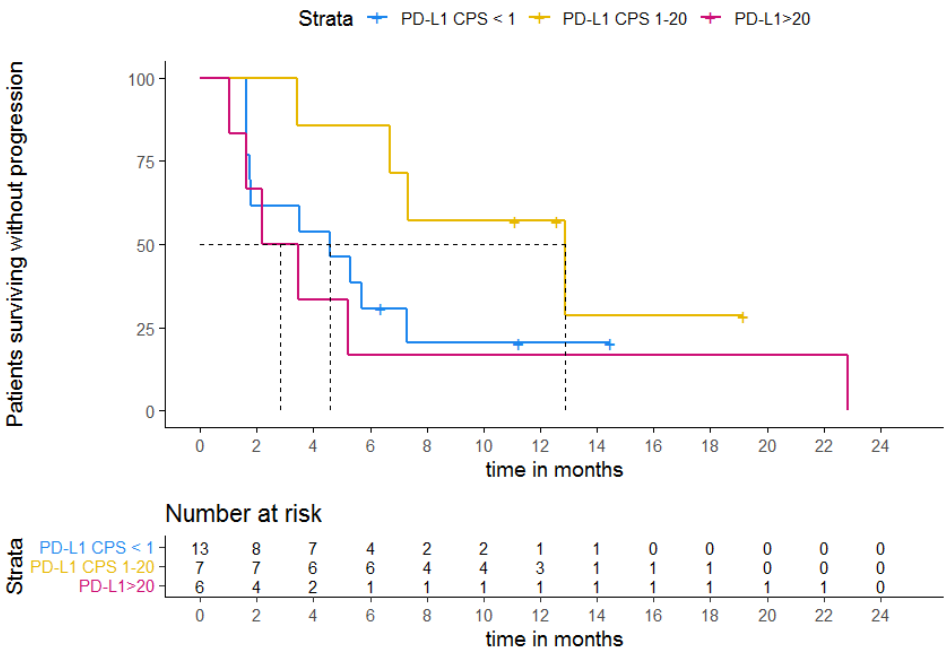

Figure 3. Association of Kaplan-Meier estimates of progression free survival with CPS score

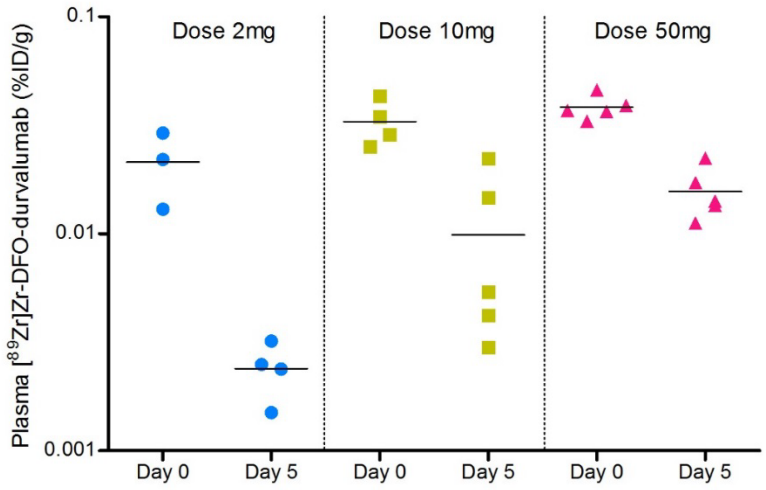

Figure 4. Pharmacokinetic analyses The percentage injected dose (%ID/g) as measured in plasma at the day of ^{89}Zr-DFO-durvalumab infusion (day 0) and at the day of PET/CT (day 5) is visualized per cohort; cohort 1 (blue dots), cohort 2 (yellow squares), cohort 3 (red triangles).

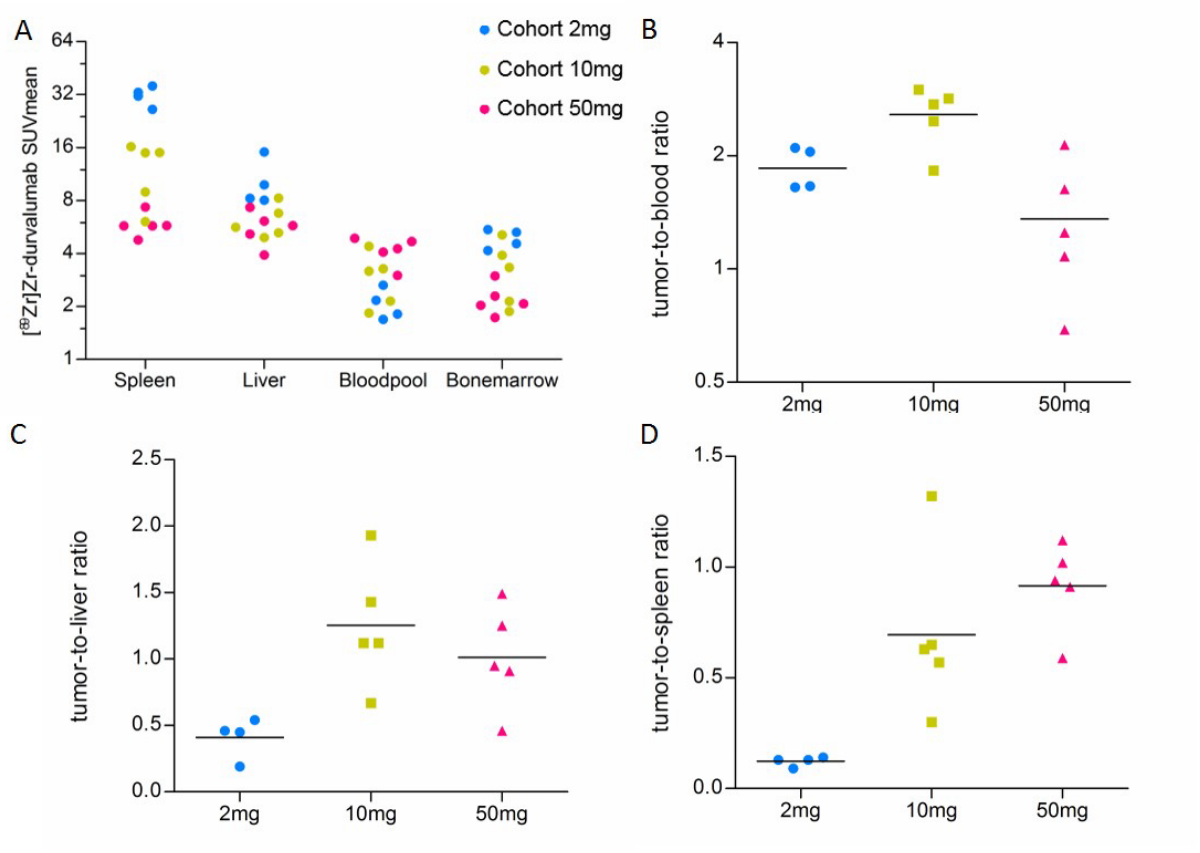

Figure 5. Quantitative analyses ^{89}Zr-DFO-durvalumab per dose cohort
The accumulation of ^{89}Zr-DFO-durvalumab in the spleen, liver, bloodpool and bone marrow for each dose cohort is shown in 4A. Cohort 2mg is resembled by blue dots, cohort 10mg by yellow squares and cohort 50mg by pink triangles**.** The subsequent tumor-to-blood (TBT) ratio, tumor-to-liver ratio and tumor-to-spleen ratios are calculated based on the SUV_{max} of the largest tumor lesion and organ SUV_{mean} values and depicted in figures 4B, 4C and 4D, respectively.

A

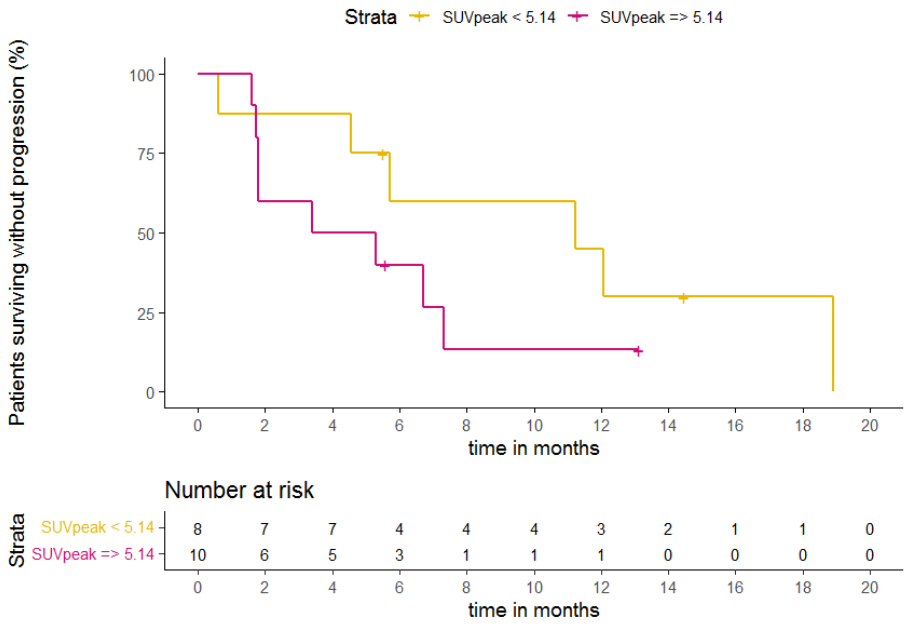

B

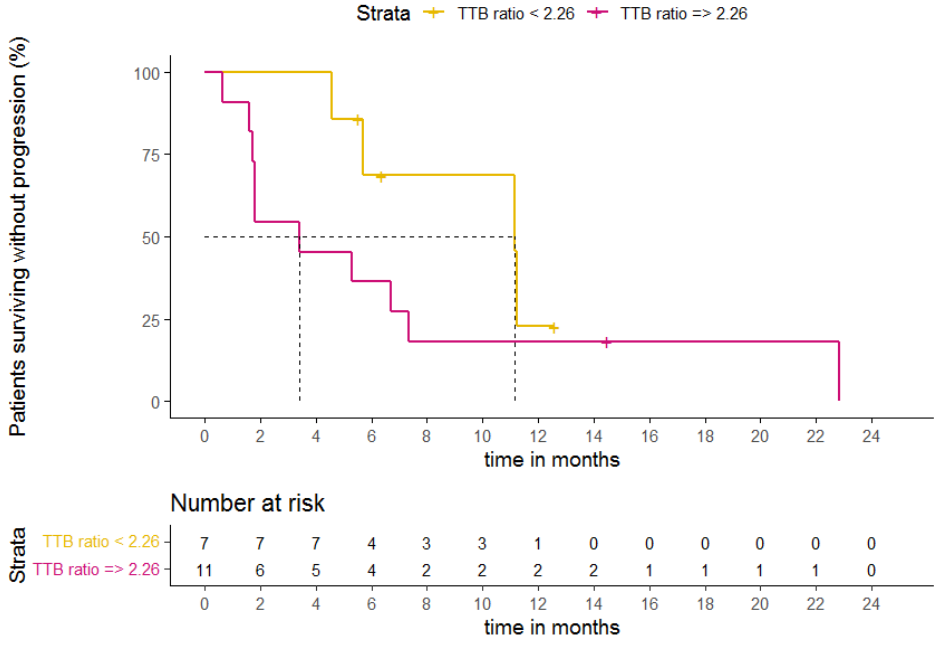

Figure 6. Kaplan-Meier estimates of progression free survival based on ^{89}Zr-DFO-durvalumab SUV_{peak} (A) and tumor-to-blood-ratios dichotomized at median value, after correcting for lesions <20mm

A

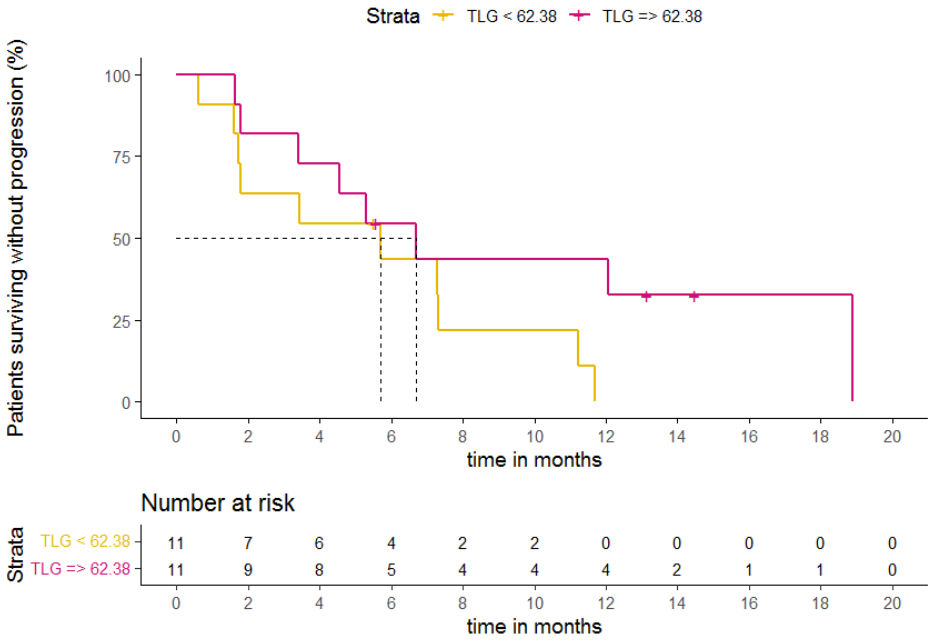

B

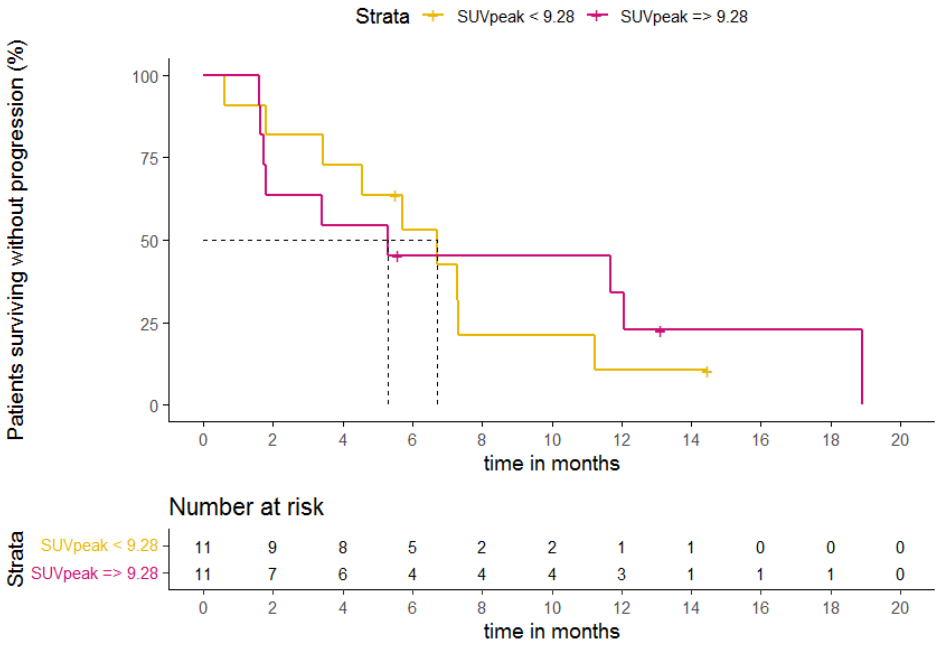

Figure 7. Kaplan-Meier estimates of progression free survival based on ^{18}F-FDG SUV_{peak} (A) and total lesion glycolysis dichotomized at median value, after correcting for lesions <20mm.

Table 1. Treatment-related adverse events (trAE) in all treated patients (N=31)				
	Any grade		**Grade 3-4**	
Patients with any trAE, n(%)	**27**	**(87%)**	**13**	**(48%)**
Bleeding	**5**	(19%)	**2**	(15%)
Diarrhea or constipation	**9**	(33%)	**-**	
Elevated AST/ALT	**6**	(22%)	**3**	(23%)
Elevated AF	**2**	(7%)	**1**	(8%)
Elevated GGT	**3**	(11%)	**1**	(8%)
Elevated creatinine (1x nephritis)	**3**	(11%)	**1**	(8%)
Fatigue	**12**	(44%)	**-**	
Hyperglycaemia	**2**	(7%)	**1**	(8%)
Hypo- or hyperthyroidism	**5**	(19%)	**-**	
Hyponatremia	**3**	(11%)	**1**	(8%)
Hearing loss	**1**	(4%)	**1**	(8%)
Peripheral sensory neuropathy	**2**	(7%)	**-**	
Myalgia	**4**	(15%)	**-**	
Rash	**3**	(11%)	**-**	
Respiratory tract (2x pneumonitis)	**13**	(48%)	**3**	(23%)
Thrombocytopenia	**1**	(4%)	**1**	(8%)

Table 1. (≥5% for any grade, ≥2% for grade 3-4)
Overall, 27 patients (87%) reported a trAE. Four patients died, of treatment unrelated event; one following a spondylodiscitis and one other patients due to trauma. Two patients died from a covid-19 infection.

Lesion no	Dose cohort	Organ	Size in CT	PET volume	FDG SUV_{max}	FDG SUV_{peak}	FDG TLG	Zr89 SUV_{max}	Zr89 SUV_{peak}	Tumor-to-blood ratio
1	2mg	Lymph node	15	2.74	17.49	12.33	27.80	3.51	2.40	2.07
2	2mg	Local recurrence	51	33.09	15.24	13.33	314.26	3.06	2.17	1.81
3	2mg	Lymph node	15	7.80	7.47	6.60	34.53	4.72	3.69	1.79
4	2mg	Lung	10	2.80	3.80	2.90	6.22	2.60	1.98	.98
5	2mg	Lung	19	10.96	6.18	5.21	36.16	2.08	1.86	.79
6	2mg	Lymph node	10	4.40	9.40	7.80	25.57	4.67	3.61	2.58
7	2mg	Lymph node	16	5.40	13.20	11.10	43.77	4.95	4.37	2.29
8	10mg	Liver	20	3.50	8.50	6.90	18.23	12.79	9.84	6.95
9	10mg	Lymph node	38	15.50	9.10	7.50	84.08	8.24	5.91	4.48
10	10mg	Adrenal gland	16	1.40	8.50	5.10	7.27	5.95	4.88	3.24
11	10mg	Lymph node	31	17.80	12.90	11.30	136.41	6.57	4.84	3.57
12	10mg	Lung	14	3.30	5.50	4.30	11.02	5.40	4.00	2.93
13	10mg	Lung	19	2.60	7.20	5.80	11.78	4.37	3.27	2.37
14	10mg	Lymph node	33	10.84	9.68	8.32	65.58	17.94	12.24	5.65
15	10mg	Lung	20	3.50	4.40	3.40	9.08	10.18	8.65	3.11
16	10mg	Lung	11	1.90	4.70	-	1.88	11.45	8.54	3.49
17	10mg	Lung	12	1.30	3.70	2.00	2.68	11.05	8.43	3.37
18	10mg	Lung	24	3.80	9.60	7.90	22.13	6.09	5.01	2.84
19	10mg	Lung	25	7.00	9.10	8.07	40.26	5.75	4.66	2.68
20	50mg	Lung	12	1.90	4.30	3.74	4.98	2.07	1.76	.51
21	50mg	Lung	12	1.60	4.60	3.50	4.52	2.00	1.74	.49
22	50mg	Local recurrence	13	3.96	6.91	4.99	15.79	5.46	4.59	1.12
23	50mg	Muscle	17	3.10	8.30	6.70	14.88	7.94	6.74	1.86
24	50mg	Muscle	21	6.00	8.30	7.80	31.03	7.32	6.39	1.72
25	50mg	Local recurrence	57	12.11	9.23	7.66	62.06	10.04	6.74	3.34
26	50mg	Lung	9	3.42	3.21	2.24	5.92	6.83	4.62	2.27
27	50mg	Lung	25	6.86	6.16	4.56	23.74	3.30	3.69	1.42
28	50mg	Lymph node	64	20.91	7.94	6.39	92.09	4.27	2.58	1.10
29	10mg	Lymph node	62	48.10	22.70	18.20	659.00	9.97	8.07	2.26
30	10mg	Lymph node	10	1.40	3.80	2.40	3.26	3.92	2.99	.89
31	50mg	Lung	31	3.98	16.63	12.01	37.28	6.28	5.59	1.34
32	50mg	Lung	47	10.95	14.10	11.00	87.04	5.92	4.94	1.27
33	10mg	Lymph node	14	8.96	7.96	6.74	41.54	7.88	5.33	7.73
34	10mg	Lymph node	42	22.02	8.30	7.80	115.45	4.56	3.28	4.47
35	10mg	Lymph node	24	6.40	9.84	8.33	36.29	3.52	2.41	3.45
36	10mg	Local recurrence	28	16.00	13.60	11.30	125.15	4.58	3.77	4.98
37	10mg	Lung	14	1.20	3.90	2.30	2.78	2.26	1.73	2.46

38	10mg	Bone	13	13.00	11.50	9.80	62.96	7.26	6.06	1.48
39	10mg	Bone	13	6.10	8.60	7.40	31.73	6.31	4.86	1.29
40	10mg	Local recurrence	18	3.55	10.67	8.20	21.54	5.07	3.85	1.03
41	10mg	Bone	33	3.40	24.10	17.80	47.11	17.04	13.39	7.42
42	10mg	Local recurrence	55	8.80	14.10	11.10	76.47	12.48	9.46	5.44
43	10mg	Local recurrence	16	6.30	6.40	5.20	22.26	8.43	6.57	2.26
44	10mg	Lung	15	2.00	6.30	4.30	7.47	8.61	7.12	2.50
45	10mg	Lung	20	3.10	5.70	4.30	10.31	5.86	3.77	1.70
46	10mg	Lymph node	35	15.80	8.20	7.10	72.26	7.41	5.80	2.66
47	10mg	Lymph node	36	6.40	6.60	5.50	24.15	5.46	4.61	1.96
48	10mg	Lung	24	7.10	6.70	5.80	28.11	6.05	4.37	2.17
49	10mg	Local recurrence	22	4.40	4.00	2.60	11.31	4.92	3.76	1.45
50	10mg	Lymph node	43	31.38	14.80	13.30	295.43	6.55	5.42	2.24
51	10mg	Lymph node	25	13.15	10.64	9.79	85.33	5.88	4.88	2.01
52	10mg	Lymph node	16	7.80	4.30	3.70	29.91	4.39	3.60	1.66
53	10mg	Lymph node	15	5.00	7.50	6.20	22.55	13.54	11.03	3.91
54	10mg	Lymph node	23	18.90	16.00	13.70	93.51	6.11	4.59	1.77
55	10mg	Local recurrence	25	8.60	7.70	6.60	39.47	5.66	4.89	1.79
56	10mg	Lung	10	1.90	5.10	4.00	5.68	2.44	2.02	.77
57	10mg	Lung	49	24.40	17.10	15.40	180.92	8.14	6.82	2.21
58	10mg	Lung	37	20.40	13.90	12.00	175.66	5.46	5.06	1.49
59	10mg	Lung	20	4.90	10.60	10.10	39.47	4.23	3.95	1.15
60	10mg	Lymph node	15	3.80	12.60	10.10	5.68	3.85	3.82	1.05
61	10mg	Lung	23	8.30	9.50	8.80	44.75	7.56	5.91	2.44
62	10mg	Lymph node	20	5.60	14.50	13.00	49.30	8.00	5.78	2.58
63	10mg	Lymph node	16	5.40	11.40	10.70	37.62	2.21	2.21	.71
64	10mg	Lung	17	5.20	5.60	5.10	17.03	1.56	1.56	.50
65	10mg	Local recurrence	29	52.00	5.90	5.40	164.66	5.90	5.11	1.61
66	10mg	Bone	34	16.70	11.80	10.20	111.76	18.07	13.64	3.58
67	10mg	Lung	70	60.00	16.60	15.10	530.02	13.76	10.78	4.29
68	10mg	Lung	10	3.30	2.70	2.30	4.96	2.80	2.11	1.55
69	10mg	Lung	16	4.40	4.70	3.80	11.57	2.42	1.84	1.35
70	10mg	Local recurrence	56	39.10	13.00	11.00	271.56	6.92	6.52	1.88

Table 2. Oversight of all FDG-positive lesions and their quantitative ^{18}F-FDG- and ^{89}Zr-DFO-durvalumab uptake. Each row represents a single lesion.